

RESEARCH ARTICLE

[View Article Online](#)  
[View Journal](#) | [View Issue](#)



Cite this: *RSC Med. Chem.*, 2025, **16**, 5333

## Development of a nitric oxide-releasing cephalaxin-based hybrid compound for enhanced antimicrobial efficacy and biofilm disruption

Sumit Kumar, <sup>a</sup> Myddelton C. Parker, <sup>a</sup> Yi Wu, <sup>a</sup> Anastasia Marx, <sup>a</sup> Hitesh Handa <sup>ab</sup> and Elizabeth J. Brisbois <sup>\*,a</sup>

Biofilm formation on medical devices and the rise of antibiotic resistance have undermined conventional antibiotics such as cephalaxin (CEX), which is effective against Gram-positive infections but has limited activity against Gram-negative pathogens and biofilms. To overcome these limitations, we developed a hybrid nitric oxide (NO)-releasing conjugate (SNAP\_CEX) by covalently attaching the NO donor *S*-nitroso-*N*-acetylpenicillamine (SNAP) to CEX. SNAP\_CEX exhibited a sustained NO release profile over 30 days, indicating enhanced stability compared to SNAP's rapid degradation, even though the Griess assay showed NO release from SNAP over 30 days. The hybrid maintained strong antibacterial activity against *Staphylococcus aureus* (*S. aureus*; MIC<sub>50</sub> = 7  $\mu$ M vs. 2.5  $\mu$ M for CEX) and dramatically improved efficacy against *Pseudomonas aeruginosa* (*P. aeruginosa*; MIC<sub>50</sub> = 3 mM vs. 16 mM for CEX). SNAP\_CEX also significantly disrupted established biofilms, reducing *S. aureus* biofilm biomass by ~75% (vs. ~33% by CEX) and viable cells by ~99%, and achieving ~67% biomass reduction and 77% killing in *P. aeruginosa* biofilms (vs. ~25% and 18% by CEX). These effects demonstrate that SNAP\_CEX combines NO's biofilm-disruptive action with antibiotic therapy to combat biofilm-associated resistant infections, while remaining cytocompatible at therapeutic concentrations.

Received 10th July 2025,  
Accepted 23rd August 2025

DOI: 10.1039/d5md00602c

[rsc.li/medchem](http://rsc.li/medchem)

### Introduction

The escalating problem of antibiotic resistance poses a substantial threat to global health since it undermines the efficacy of conventional therapies and results in elevated rates of morbidity and mortality caused by bacterial infections.<sup>1,2</sup> Bacterial pathogens increasingly develop resistance and flexibility, making conventional antimicrobial treatments such as antibiotic therapy less effective.<sup>3–7</sup> Cephalaxin (CEX) is an FDA-approved, first-generation  $\beta$ -lactam antibiotic used to treat various streptococcal and staphylococcal infections.<sup>8</sup> The drug is administered orally to treat bone, skin, and soft tissue infections caused by *Staphylococcus aureus* (*S. aureus*). However, the drug is limited in its effectiveness against Gram-negative strains, such as *Pseudomonas aeruginosa* (*P. aeruginosa*).<sup>9–11</sup> Compounding the issue, these Gram-negative strains, similar to Gram-positive strains, are often biofilm-forming, creating an additional barrier to treatment.<sup>12,13</sup>

Biofilms are complex microbial communities embedded in a self-produced extracellular matrix. This matrix shields bacteria from the immune system and antimicrobial agents, contributing to increased resistance and persistence of infections in clinical settings.<sup>14–17</sup> Therefore, enhancing the antibacterial profile of CEX to disrupt biofilms and broaden its efficacy spectrum to include Gram-negative pathogens is crucial.

One promising approach to overcoming these limitations involves coupling antibiotics with biofilm-disruptive agents, such as nitric oxide (NO)-releasing compounds. Nitric oxide is a small, reactive molecule known for its broad-spectrum antimicrobial activity and unique properties that disrupt biofilms. The ability of NO to penetrate biofilms and disrupt bacterial cell membranes makes the bacterial cells more susceptible to antibiotics.<sup>18,19</sup> It disrupts biofilm integrity, enabling enhanced antibiotic penetration and reducing biofilm defenses, while antibiotics such as CEX target bacterial proliferation.<sup>20,21</sup> Compared to penicillins, cephalosporins such as CEX generally exhibit a broader antibacterial spectrum, improved pharmacokinetic profiles, and greater stability against many  $\beta$ -lactamases.<sup>22,23</sup> These attributes make them valuable in treating infections caused by  $\beta$ -lactamase-producing strains and mixed Gram-positive/Gram-negative infections where penicillins may be less effective. Building on previous work with the NO-

<sup>a</sup> School of Chemical, Materials, and Biomedical Engineering, College of Engineering, University of Georgia, Athens, GA 30602, USA.

E-mail: [ejbrisbois@uga.edu](mailto:ejbrisbois@uga.edu)

<sup>b</sup> Pharmaceutical and Biomedical Science Department, College of Pharmacy, University of Georgia, Athens, GA 30602, USA



releasing ampicillin conjugate ("SNAPicillin"),<sup>24</sup> the use of CEX in the present study aimed to enhance Gram-negative coverage and maintain Gram-positive activity while leveraging the biofilm-disruptive effects of NO. The combined attack of NO and antibiotics inhibits the bacteria's ability to adapt and survive, enhancing the therapy's overall efficacy.<sup>25</sup>

S-Nitroso-*N*-acetylpenicillamine (SNAP) is a well-studied NO donor that releases NO in a controlled and prolonged fashion.<sup>26</sup> This tunable release considerably enhances its ability to kill bacteria, as the regulated discharge guarantees an extended period of effectiveness against bacteria, minimizing the likelihood of rapid bacterial adaptation and the development of resistance.<sup>27</sup> SNAP's wide-ranging qualities render it very efficient against many bacterial strains. The compound's potential to disturb biofilms and its ability to provide a protective shield against bacterial colonies enhances its efficacy in treating persistent illnesses.<sup>28</sup> The other significant advantage of using SNAP is that it's a derivative of the FDA-approved *N*-acetyl penicillamine.<sup>29</sup>

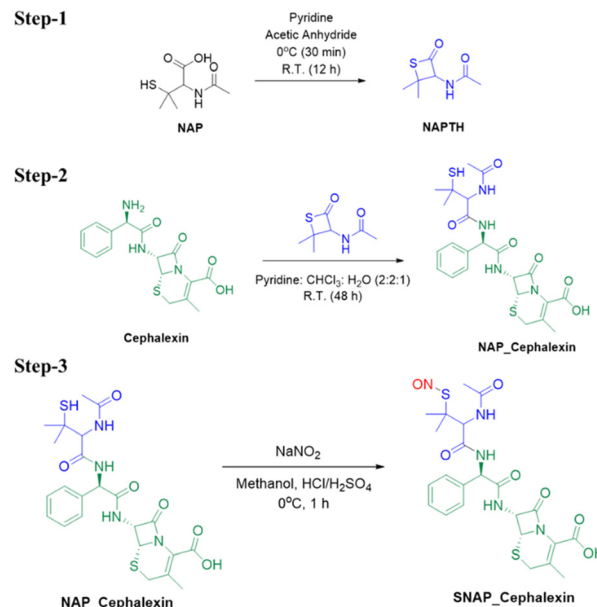
Therefore, combining SNAP with antibiotics is a promising approach to enhancing the efficacy of biofilm disruption and maintaining the effectiveness of current therapies. The objectives of this study include synthesizing a new molecule that covalently conjugates SNAP to the antibiotic cephalexin (SNAP\_CEX), characterizing its NO release profile, and evaluating its antibacterial and biofilm disruption efficacy against Gram-positive (*S. aureus*) and Gram-negative (*P. aeruginosa*) strains. This study addresses two critical limitations of CEX: its limited activity against Gram-negative pathogens and its restricted capacity for biofilm disruption. These results advance the development of antibiotics targeting biofilms, providing a therapeutic strategy that combines direct antibacterial action with inhibition of biofilm formation for applications in treating complex infections and reducing biofilm-related risks in clinical and biomedical settings.

## Result and discussion

### Chemical modification of antibiotic, cephalexin (CEX) and its characterizations

Previously, our group developed SNAPicillin, a compound that combines SNAP with ampicillin, which showed improved biofilm disruption and antibacterial activity.<sup>24</sup> In the current study, SNAP\_CEX offers specific advantages over SNAPicillin. CEX offers a broader antibacterial spectrum than ampicillin, enabling SNAP\_CEX to target both Gram-positive and Gram-negative bacteria effectively.<sup>22,23</sup> To synthesize SNAP\_CEX, a tertiary RSNO group was covalently attached to CEX using a two-step process involving *N*-acetyl-*D*-penicillamine (NAP) and its thiolactone derivative (Scheme 1, step 1). First, NAP was converted into its self-protected thiolactone form, 3-acetamido-4,4-dimethylthietan-2-one (NAPTH), following the reported methodology.<sup>30</sup>

Next, the NAP group was attached to CEX through aminolysis of NAPTH (Scheme 1, step 2). CEX was mixed with an equimolar amount of NAPTH in a 2:1:1 (pyridine:chloroform:water)



**Scheme 1** The schematic representation of the chemical modification of CEX with NO donor SNAP. Step 1: conversion of NAP and its thiolactone derivative, NAPTH. Step 2: NAP group was attached to CEX through aminolysis of NAPTH. NAP\_CEX was obtained using vacuum filtering and desiccated under vacuum. Step 3: NAP\_CEX was dissolved in methanol to induce nitrosation, and the synthesis was carried out in acidic conditions using 1 M HCl and concentrated H<sub>2</sub>SO<sub>4</sub>. SNAP\_CEX product was collected by vacuum filtration, stored at -20 °C, and protected from light.

ratio and stirred at room temperature for 48 h. Following the removal of the solvent using rotary evaporation, the impure product was dissolved again in chloroform (30 mL), subjected to three washes with 1 M HCl, and then dehydrated using magnesium sulfate. The product was finally purified through recrystallization in hexane. The NAP\_CEX was obtained using vacuum filtering and desiccated under vacuum. NAP\_CEX was dissolved in methanol to induce nitrosation, and the synthesis was carried out in acidic conditions using 1 M HCl and concentrated H<sub>2</sub>SO<sub>4</sub> as per the reported literature (Scheme 1, step 3).<sup>31</sup> The resulting SNAP\_CEX product was collected by vacuum filtration, stored at -20 °C, and protected from light.

To confirm the synthesis of the desired compound, the NAP\_CEX (intermediate) and the final nitrosated compound were characterized with the help of proton nuclear magnetic resonance (NMR), carbon NMR, distortionless enhancement by polarization transfer (DEPT) NMR, and electrospray ionization mass spectrometry (ESI-MS) analysis. The results of these analyses are provided in Fig. S1–S6 of the SI. The study conducted on NAP\_CEX in DEPT-45 revealed that all the carbon atoms in the molecule that lacked a proton were no longer visible in the spectrum, as seen in Fig. S7a. Similarly, the DEPT-135 analysis verified the presence of only one CH<sub>2</sub> group in the molecule, as evidenced by a single negative signal in the study (Fig. S7b).

The proton NMR comparison between the intermediate and final desired product indicated that the thiol group had



been fully converted to the nitroso group. Fig. S8a and b clearly illustrates the total disappearance of the peak at 2.8, which corresponds to the proton of the thiol group following the nitrosation phase. The ESI-MS analysis revealed a difference of 29 in the reported mass of both compounds. This difference may be attributable to the fact that the NO group has a mass of 30 (14 for N and 16 for O), whereas the hydrogen atom has a mass of 1. During the conversion process, the hydrogen atom is removed, and the presence of the nitroso group is indicated by a mass change of 29 (Fig. S8c and d). Overall, the synthesis of the target chemical was thoroughly and comprehensively characterized.

### Nitric oxide quantification using the Griess assay

Griess assay is the most frequent colorimetric method for measuring NO *via* its stable metabolite, nitrite ( $\text{NO}_2^-$ ), in biological samples.<sup>32</sup> Given the high reactivity of NO and its very short half-life, it quickly oxidizes to nitrite in aqueous solutions, allowing for indirect quantification.<sup>33</sup>

For the analysis, 10  $\mu\text{L}$  of each SNAP and SNAP\_CEX solutions were used, with concentrations ranging from 3000  $\mu\text{M}$  to 4.8  $\mu\text{M}$ . Measurements were taken at days 1, 5, 14, 21, and 30 (Fig. 1a). The highest concentration (3 mM) of SNAP\_CEX released approximately 45–55  $\mu\text{g mL}^{-1}$  of nitrite on day 1, with sustained levels maintained through day 21. At 600  $\mu\text{M}$ , a concentration more relevant for *in vitro* biological applications, a striking contrast emerged between SNAP\_CEX and the parent SNAP compound (Fig. 1b). As the Griess assay measures accumulated nitrite ( $\text{NO}_2^-$ ), the slope of the curve between timepoints provides a more meaningful estimate of the NO release rate over time. We therefore calculated the average daily NO release for each interval by subtracting consecutive nitrite values and dividing by the number of days in that interval. The resulting values (Table S1, SI) indicate that SNAP\_CEX exhibited the highest daily release between days 1–5 (8.53  $\mu\text{g mL}^{-1}$  per day; 185  $\mu\text{M}$  per day), followed by a gradual decline over the subsequent intervals, yet maintaining measurable release up to day 28. SNAP displayed a similar trend but with lower daily release values at all timepoints. The enhanced stability of the RSNO group in SNAP\_CEX is likely attributed to the CEX scaffold, which may provide electronic or steric shielding, slowing the rate of S-NO bond cleavage and reducing premature

conversion to disulfide (RSSR).<sup>34,35</sup> To further investigate stability, additional analyses were conducted to examine the stability differences between SNAP\_CEX and SNAP, which are elaborated upon in the following section.

### NMR and UV stability

The investigation on NO quantification for SNAP\_CEX showed that the compound exhibited higher NO release than SNAP. This prompted an investigation into its stability over an extended period at room temperature. A detailed  $^1\text{H}$  NMR analysis was conducted to assess this and monitor any potential degradation for both compounds over 30 days, stored at room temperature under dark conditions. The stability investigation collected  $^1\text{H}$  NMR spectra at certain time intervals: 0, 1, 2, 7, 14, 21, and 30 days. This approach enabled us to monitor any changes in the chemical composition of SNAP\_CEX over time, which would suggest degradation or instability. This study addresses the instability of SNAP, a promising NO-releasing antibacterial agent that degrades rapidly at room temperature. By modifying SNAP to form SNAP\_CEX, the research aims to enhance its stability and shelf life, ensuring sustained NO release and efficacy. This approach provides a pathway for developing more robust and reliable antibacterial therapies.

Throughout the 30 days, new samples were prepared each time after dissolving the stored solid sample in deuterated DMSO. The  $^1\text{H}$  NMR spectra were carefully analyzed for shifts in peak positions, changes in peak intensities, or the appearance of new peaks, all of which could signal chemical degradation or the formation of decomposition products. The results demonstrated that SNAP\_CEX maintained its structural integrity throughout the observation period (Fig. 2a), with no significant changes observed in the  $^1\text{H}$  NMR spectra. This stability suggests that the compound can remain effective and reliable when stored at room temperature for at least 30 days.

However, SNAP began to show instability on the 21st day, as indicated by the appearance of peaks 1, 2, and 3 in the  $^1\text{H}$  NMR spectrum (Fig. 2b). This peak further intensifies on day 30, showing the instability of SNAP over the hybrid compound SNAP\_CEX. These changes correspond to the protons at specific positions within the SNAP molecule and suggest the formation of disulfide products (RSSR).

Ketchum *et al.* has reported a similar result regarding the degradation of the SNAP molecule, as it is temperature-sensitive.<sup>36</sup> Interestingly, as discussed above, upon modification with the drug to form the hybrid molecule, it was found that this compound remained stable for up to 30 days, significantly extending its shelf life compared to SNAP alone, which was only stable for 14 days.

Further, to analyze the stability of both SNAP and SNAP\_CEX, a UV-stability study was conducted for the solid stored sample at room temperature. The degradation of the compound peak at 590 nm in the UV spectrum was monitored for NO, as NO shows peaks at 340 nm and 590 nm. The peak at 340 nm is associated with a  $\pi \rightarrow \pi^*$  transition, while the peak at

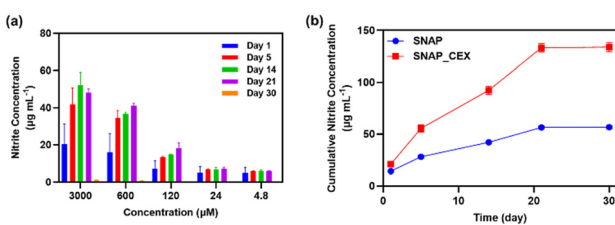


**Fig. 1** Nitrite release profiles of SNAP\_CEX and SNAP measured by Griess assay. (a) SNAP\_CEX shows sustained NO release across concentrations (3000–4.8  $\mu\text{M}$ ) over 30 days. (b) At 600  $\mu\text{M}$ , SNAP\_CEX displays a steady increase in nitrite levels (cumulative) over time as compared to SNAP.



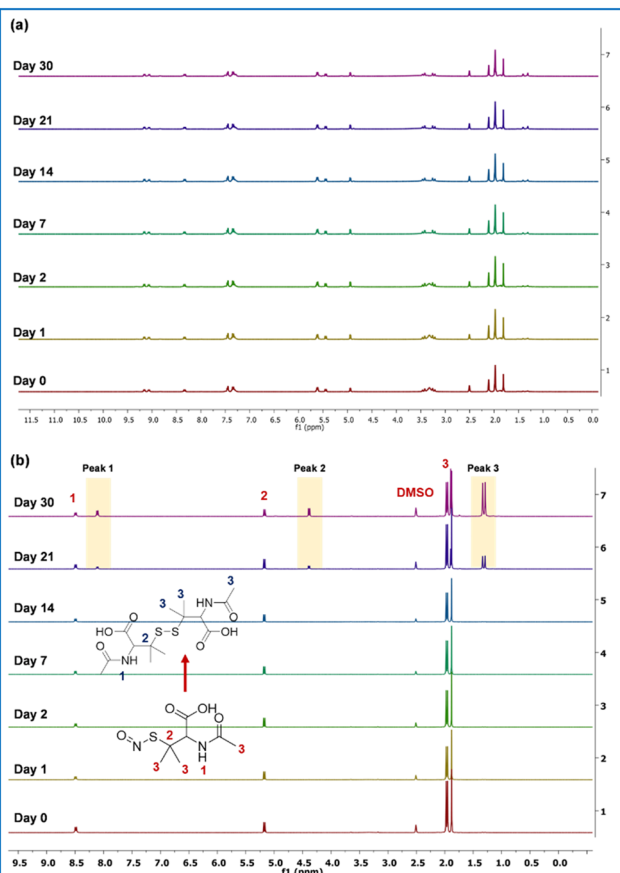


**Fig. 2** (a)  $^1\text{H}$  NMR spectra of SNAP\_CEX recorded at room temperature in dark conditions over 30 days. The spectra were taken at intervals of 0, 1, 2, 7, 14, 21, and 30 days to monitor potential degradation. (b)  $^1\text{H}$  NMR spectra of SNAP recorded at room temperature over 30 days. The spectra showed degradation on the 21st day, and further degraded within 30 days.

590 nm corresponds to an  $n \rightarrow \pi^*$  transition. The reason for monitoring the 590 nm peak is that it does not interfere with the absorption of drug CEX, facilitating comparative analysis. The data were collected for days 1, 2, 7, 14, 21, and 28 for both compounds, indicating that SNAP (Fig. 3a) showed a degradation of 19% compared to only a 4% degradation of SNAP\_CEX (Fig. 3b) in the NO peak. The stability of the drug-hybrid molecule suggests that the hybridization effectively mitigates the degradation pathways that plague SNAP, providing

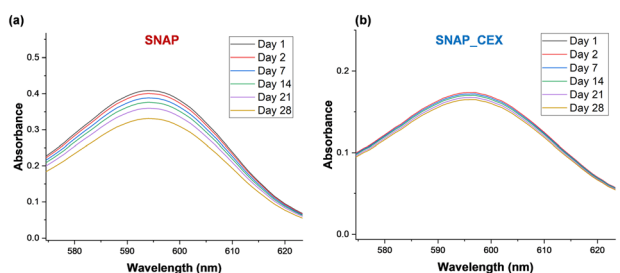


**Fig. 3** UV-vis absorbance spectra of (a) SNAP and (b) SNAP\_CEX at 590 nm measured over 28 days to assess NO stability.

a promising avenue for developing more robust antibacterial agents.

### Minimum inhibitory concentration (MIC) determination

The Gram-positive bacterium *Staphylococcus aureus* (*S. aureus* ATCC 6538) and the Gram-negative bacterium *Pseudomonas aeruginosa* (*P. aeruginosa* ATCC 9027) used for MIC determination were obtained from the American Type Culture Collection (ATCC) located in Manassas, Virginia. The MIC of the newly developed SNAP\_CEX hybrid compound was assessed to determine its antibacterial effectiveness compared to the drug CEX, a widely used antibiotic, and SNAP, the NO donor used in the modification. The bacterial growth of Gram-positive *S. aureus* and Gram-negative *P. aeruginosa* was monitored by measuring the absorbance of bacterial solutions in 96-well plates over 24 h. Absorbance values were plotted against treatment concentrations after 24 h of treatment, and  $\text{MIC}_{50}$  values were calculated as the concentration required to reduce bacterial growth by 50% relative to controls.

When treating *S. aureus*, CEX had the highest antimicrobial efficacy at the lowest concentration (Fig. 4a). CEX's  $\text{MIC}_{50}$  value was 2.5  $\mu\text{M}$ , whereas SNAP conjugated hybrid compound (SNAP\_CEX; Fig. 4c) required 7  $\mu\text{M}$ , and SNAP achieved 50%

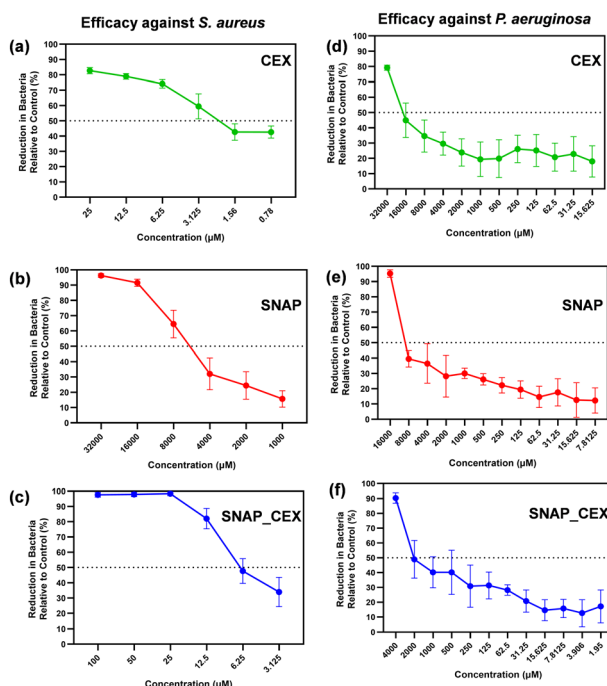


**Fig. 4** Minimum inhibitory concentration ( $\text{MIC}_{50}$ ) assessment of SNAP\_CEX hybrid compound compared to CEX and SNAP. (a–c)  $\text{MIC}_{50}$  evaluation against Gram-positive *S. aureus*: (a) CEX shows the highest efficacy with an  $\text{MIC}_{50}$  of 2.5  $\mu\text{M}$ , (b) SNAP with an  $\text{MIC}_{50}$  of 5–6 mM, and (c) SNAP\_CEX with an  $\text{MIC}_{50}$  of 7  $\mu\text{M}$ . (d–f)  $\text{MIC}_{50}$  evaluation against Gram-negative *P. aeruginosa*: (d) CEX with an  $\text{MIC}_{50}$  of 16 mM, (e) SNAP with an  $\text{MIC}_{50}$  of 8–10 mM, and (f) SNAP\_CEX demonstrates superior efficacy with an  $\text{MIC}_{50}$  of 3 mM. The values were measured at 24 h and plotted against treatment concentrations. Data represent three independent assays' mean and S.D.

killing at 5–6 mM concentration (Fig. 4b). This result is expected to be higher for the CEX because it is well-known for its potential against the Gram-positive strain of bacteria. Therefore, modifying the compound results in a slight reduction in efficacy against the same strain, possibly due to alterations in the amine group, a key component for drug interactions with *S. aureus*.<sup>37</sup>

Next, all three compounds were evaluated against *P. aeruginosa*; SNAP\_CEX demonstrated a reduction in bacterial growth at concentrations significantly lower than those of both CEX and SNAP. The MIC<sub>50</sub> value for SNAP\_CEX was determined to be 3 mM (Fig. 4f), while CEX (Fig. 4d) and SNAP (Fig. 4e) required 16–18 mM and 8–10 mM, respectively, to achieve the same effect. Similarly, the graphs plotted here are combinations of three different assays.

Additionally, the results obtained for SNAP alone were consistent with previous studies on the antimicrobial properties of SNAP in solution.<sup>24</sup> The effectiveness of SNAP\_CEX as an antimicrobial agent was evident only when SNAP was combined with CEX. These results align with the existing literature,<sup>18,38</sup> indicating that combining NO-releasing moieties with traditional antibiotics reduces bacterial resistance to antimicrobial treatments and slows the development of antibiotic resistance.

To further explore whether the NO donor and the  $\beta$ -lactam scaffold exhibit complementary effects when present together, a checkerboard assay was performed using SNAP and CEX as separate agents, and the fractional inhibitory concentration (FIC) index was calculated. Because SNAP\_CEX is a single covalently linked hybrid molecule, the FIC method is not directly applicable to its activity; however, examining the parent compounds in combination provides useful context for interpreting the hybrid's performance. The checkerboard results, presented in the SI (Fig. S10), suggest a potential for synergy between SNAP and CEX, particularly against *S. aureus*, supporting the rationale for covalently linking these two functional components into a single, stable molecular framework.

### Biofilm reduction assay

Biofilms are structured bacterial communities encased in a protective extracellular polymeric substance (EPS) matrix that limits antibiotic penetration and shields bacteria from immune defenses, making infections difficult to treat.<sup>39,40</sup> Biofilm formation involves initial attachment, maturation into a resistant matrix, and dispersal, allowing for the spread of infection and requiring high antibiotic doses with potential toxicity.<sup>41</sup> Past studies have indicated that using CEX alone is ineffective in disrupting biofilm infections.<sup>42,43</sup> The use of NO offers a promising alternative, as it can penetrate biofilms, destabilize the EPS, and induce bacterial dispersal, thereby making the bacteria more amenable to treatment.<sup>44</sup> Therefore, NO-donor compounds, such as SNAP\_CEX, combine NO's penetrative and biofilm-disruptive properties with the antimicrobial activity of cephalexin to provide a superior solution over traditional treatments.

To further investigate the antibiofilm efficacy of the NO-releasing antibiotic conjugate, SNAP\_CEX, we evaluated its performance against robust biofilms of *S. aureus* and *P. aeruginosa* using three complementary assays: crystal violet staining for total biofilm biomass, colony-forming unit (CFU) enumeration for biofilm viability, and planktonic bacterial viability. Biofilms were grown for 48 h on thin film substrates, followed by a 24 h treatment with CEX, NO donor (SNAP), or the hybrid compound SNAP\_CEX. Treated samples were analyzed according to assay-specific workflows as outlined in the schematic (Fig. 5a).

Crystal violet (CV) staining, used to quantify total biofilm biomass including the extracellular matrix, revealed that SNAP\_CEX significantly disrupted both *S. aureus* and *P. aeruginosa* biofilms. In the case of *S. aureus*, SNAP\_CEX resulted

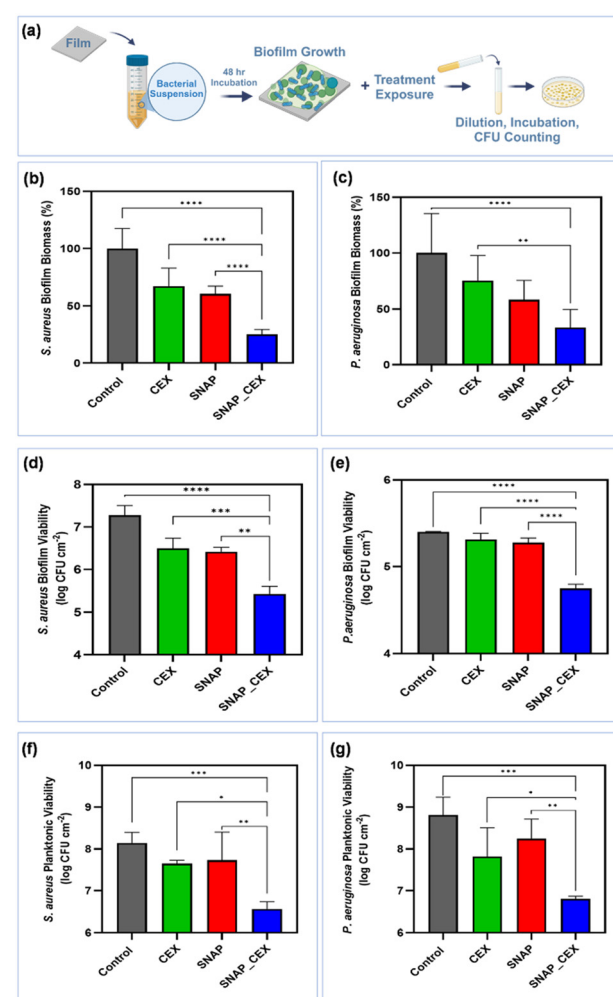


**Fig. 5** Evaluation of the antibiofilm activity of CEX, SNAP, and SNAP\_CEX against *S. aureus* and *P. aeruginosa* biofilms. (a) Schematic of the experimental workflow showing biofilm growth, treatment, and analysis. (b and c) Biofilm biomass reduction was measured by crystal violet staining. (d and e) The biofilm viability, as determined by the colony-forming unit (CFU), counts after a disruption. (f and g) Planktonic bacterial viability from surrounding media. SNAP\_CEX showed the highest reduction in biomass and bacterial survival, highlighting its strong biofilm-disruptive and antibacterial effect.



in a 74.87% reduction in biomass compared to only 32.73% and 39.57% for CEX and SNAP, respectively (Fig. 5b). Similarly, for *P. aeruginosa*, SNAP\_CEX led to a 66.60% biomass reduction, notably higher than that of CEX (24.62%) and SNAP (41.63%) (Fig. 5c). These results suggest that SNAP\_CEX effectively breaks down the protective EPS matrix, facilitating the removal of structural components of the biofilm.

To assess the ability of the treatments to kill viable bacteria within the biofilm, treated biofilms were disrupted through mechanical homogenization, and CFUs were quantified. The SNAP\_CEX compound again demonstrated superior performance. For *S. aureus*, SNAP\_CEX achieved a 98.68% reduction in viable cells, as compared to 82.94% and 87.36% reductions with CEX and SNAP, respectively (Fig. 5d). Against *P. aeruginosa*, SNAP\_CEX resulted in a 77.65% reduction in biofilm-associated CFUs, whereas CEX and SNAP achieved reductions of 24.31% and 17.90%, respectively (Fig. 5e). This significant improvement in bacterial killing within the matrix underscores the dual action of SNAP\_CEX, where NO facilitates matrix penetration and dispersal, thereby enhancing antibiotic access and bactericidal activity.

Planktonic viability, measured by quantifying CFUs in the surrounding media, provided additional insight into the compound's effectiveness against non-adherent bacteria. SNAP\_CEX showed the highest reduction in planktonic CFUs: 97.53% for *S. aureus* and 99.25% for *P. aeruginosa*. In contrast, CEX reduced planktonic viability by 71.34% and 83.59%, while SNAP achieved reductions of 65.37% and 71.49% for *S. aureus* and *P. aeruginosa*, respectively (Fig. 5f and g). These findings demonstrate that SNAP\_CEX not only disrupts and kills biofilm-resident bacteria but also effectively eliminates bacteria that may have detached and remained suspended in the medium—an essential factor in preventing reinfection or regrowth of biofilms.

This action is further supported by confocal images (Fig. S9a and b), which demonstrate the extensive disintegration of the biofilm structure and the presence of lysed bacterial cells following treatment. It can be seen from the confocal image that significantly fewer bacterial cells are visible in SNAP\_CEX.

Scanning electron microscopy (SEM) was used to observe how *S. aureus* (Fig. 6a–h) and *P. aeruginosa* (Fig. 6i–p) biofilms respond to different treatments, CEX, SNAP, and the conjugate SNAP\_CEX (Fig. 6). In the control samples (Fig. 6a, e, i, and m), both bacteria formed dense, multi-layered biofilms with a well-developed EPS matrix, which protects the bacteria and helps them adhere to surfaces. Treatment with CEX (Fig. 6b, f, j, and n) resulted in a slight reduction in bacterial density; however, the overall biofilm structure remained largely intact. The EPS was still clearly visible, suggesting limited penetration of the antibiotic through the matrix. With SNAP alone, a more noticeable disruption was observed. The biofilm architecture appeared looser and less compact, with signs of EPS breakdown. This indicates that NO released from SNAP can disturb the matrix, likely making bacteria more exposed, but not entirely eliminating them. The most prominent effect was seen with SNAP\_CEX treatment. Here, the biofilm was almost

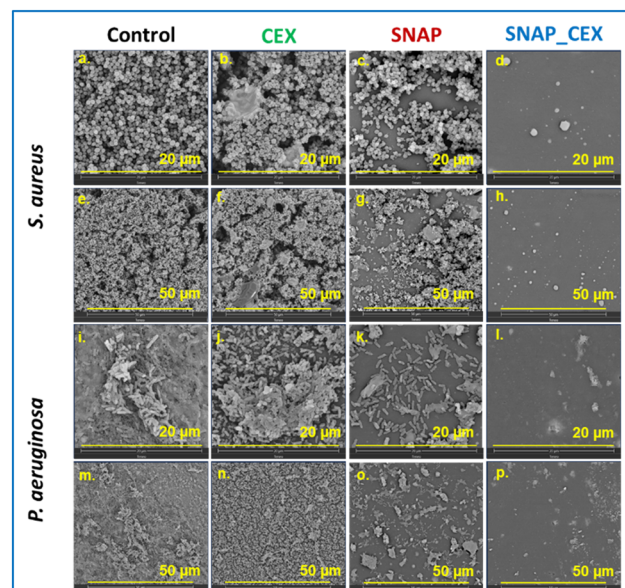


Fig. 6 Scanning electron microscopy (SEM) images showing the morphological changes in *S. aureus* (top two rows, a–h) and *P. aeruginosa* (bottom two rows, i–p) biofilms after treatment with CEX, SNAP, and SNAP\_CEX. The images show that SNAP\_CEX causes the most visible breakdown of the biofilm and removal of bacteria compared to the other treatments.

completely cleared, with very few bacteria visible. The surface appeared smooth and clean, suggesting a dual action: NO breaks up the protective biofilm barrier, and CEX then effectively kills the exposed bacteria.

Overall, these assays confirm that while SNAP alone can weaken the biofilm, the SNAP\_CEX combination leads to superior disruption and bacterial clearance in both Gram-positive and Gram-negative strains. Therefore, SNAP\_CEX offers a significant advantage in both biofilm models, particularly in breaking down the biofilm matrix and eradicating embedded bacteria.

### Biocompatibility evaluation

The human fibroblast cells used to evaluate the biocompatibility were obtained from ATCC (BJ CRL-2522). To ensure that antibiotics do not cause cytotoxicity or any other unanticipated side effects, evaluating their antimicrobial effectiveness in conjunction with their *in vitro* cytocompatibility is essential. This ensures that antibiotics may be safely applied in clinical settings. Accordingly, the cytocompatibility of the newly developed hybrid chemical, SNAP\_CEX, was assessed and compared to both CEX and SNAP.

Regarding biofilm reduction for Gram-negative organisms, the optimal concentration for biofilm treatment with all three compounds was 3 mM. Therefore, based on this, compounds should not exhibit any apparent toxicity at this concentration; all three compounds were evaluated at the highest concentration of 8 mM. The experiment's findings indicated that SNAP\_CEX and CEX exhibited equivalent outcomes in mammalian cells. At the maximum concentration of 8 mM,



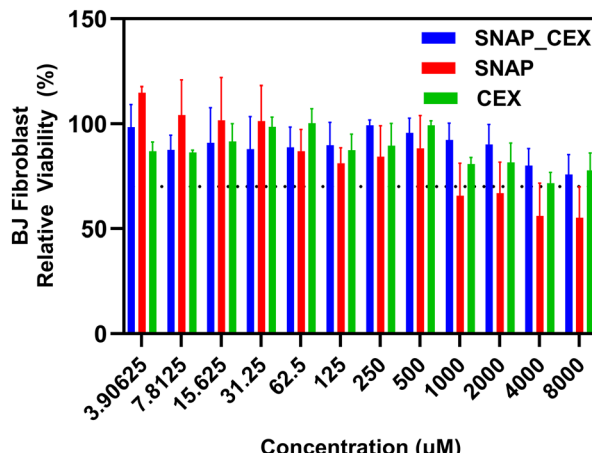


**Fig. 7** Comparative cytocompatibility evaluation of SNAP\_CEX, SNAP, and CEX at different concentrations in human fibroblast cells. The plot is the combined plot for triplicate.

each compound exhibited more than 70 percent viability. Compared to this, SNAP showed reduced cell viability at a concentration of 2 mM, indicating a more severe level of cytotoxicity (Fig. 7). The SNAP\_CEX hybrid molecule has been demonstrated to exhibit increased cytocompatibility at biologically relevant doses, as noted in this comparison.

## Conclusions

This study introduced a covalently bound NO-releasing CEX conjugate, SNAP\_CEX, and demonstrated its significantly enhanced antimicrobial and antibiofilm performance over the parent antibiotic. By integrating an NO donor onto CEX, we addressed the antibiotic's two major limitations – its lack of Gram-negative efficacy and inability to penetrate and eradicate biofilms. SNAP\_CEX displayed sustained nitric oxide release and greatly improved stability relative to SNAP alone, ensuring prolonged bactericidal activity in solution. Biological evaluations showed that SNAP\_CEX was more effective against *P. aeruginosa* compared to CEX and SNAP individually, and retained considerable activity against *S. aureus*. Notably, SNAP\_CEX exhibited superior biofilm disruption and bacterial clearance across both Gram-positive and Gram-negative models. Importantly, SNAP\_CEX showed favorable cytocompatibility at therapeutic concentrations, suggesting its potential for biomedical applications.

In its current form, SNAP\_CEX is intended for localized delivery rather than systemic oral administration. Although NO has a short half-life *in vivo*, covalent conjugation to CEX markedly prolongs NO release and stability, as confirmed by 30-day NO release and stability data. This sustained release profile makes SNAP\_CEX particularly suitable for incorporation into targeted delivery platforms such as antimicrobial medical device coatings, topical dressings, or implantable materials, where localized NO delivery can prevent or eradicate biofilm-associated infections. Such applications overcome the

limitations of systemic NO therapy while leveraging the synergistic antibacterial benefits of NO and CEX, paving the way for clinically relevant biofilm-targeted therapies.

## Author contributions

S. K., H. H., and E. J. B. conceptualized, executed, analyzed data, and drafted the manuscript. S. K. has carried out the synthesis and characterization. M. C. P., Y. W., and A. M. executed the biological experiments. All the authors participated in data analysis.

## Conflicts of interest

The authors declare the following competing financial interest(s): Hitesh Handa and Elizabeth J. Brisbois are co-founders and maintain a financial interest in a startup company investigating nitric oxide as a biomedical therapeutic for medical devices.

## Data availability

Supplementary information is available. See DOI: <https://doi.org/10.1039/D5MD00602C>.

Data will be made available upon a reasonable request.

## Acknowledgements

Funding for this work was supported by the National Institutes of Health, USA, grant R01HL172496. The graphical abstract was created in part with <https://BioRender.com>.

## Notes and references

- 1 M. A. Salam, M. Y. Al-Amin, M. T. Salam, J. S. Pawar, N. Akhter, A. A. Rabaan and M. A. A. Alqumber, *Healthcare*, 2023, **11**, 1946.
- 2 L. J. V. Piddock, Y. Alimi, J. Anderson, D. de Felice, C. E. Moore, J.-A. Röttingen, H. Skinner and P. Beyer, *Nat. Med.*, 2024, **30**, 2432–2443.
- 3 G. Muteeb, M. T. Rehman, M. Shahwan and M. Aatif, *Pharmaceutics*, 2023, **16**, 1615.
- 4 C. R. MacNair, S. T. Rutherford and M.-W. Tan, *Nat. Rev. Microbiol.*, 2024, **22**, 262–275.
- 5 K. Hu, Z. Yang, Y. Zhao, Y. Wang, J. Luo, B. Tuo and H. Zhang, *Langmuir*, 2022, **38**, 5924–5933.
- 6 Antimicrobial resistance (<https://www.who.int/news-room/fact-sheets/detail/antimicrobial-resistance>), (accessed Oct. 10, 2024).
- 7 P. Sarkar, W. Xu, M. Vázquez-Hernández, G. Dhanda, S. Tripathi, D. Basak, H. Xie, L. Schipp, P. Dietze, J. E. Bandow, N. N. Nair and J. Haldar, *Chem. Sci.*, 2024, **15**, 16307–16320.
- 8 M. Kanan, S. Atif, F. Mohammed, Y. Balahmar, Y. Adawi, R. AlSaleem, A. Farhan, M. Alghoribi, S. Mohammed, R. Alshanbari, M. Fahad, R. Kallab, R. Mohammed, D. Alassaf and A. Hazza, *Antibiotics*, 2023, **12**, 1402.
- 9 A. M. Jawad, N. M. Aljamali and M. Aseel, *International Journal of Psychosocial Rehabilitation*, 2020, **24**, 3754–3767.



10 S. H. Schneider, J. Kozuch and S. G. Boxer, *ACS Cent. Sci.*, 2021, **7**, 1996–2008.

11 J. M. Turner, K. L. Connolly, K. E. Aberman, J. C. Fonseca, II, A. Singh, A. E. Jerse, R. A. Nicholas and C. Davies, *ACS Infect. Dis.*, 2021, **7**, 293–308.

12 R. Mirghani, T. Saba, H. Khaliq, J. Mitchell, L. Do, L. Chambi, K. Diaz, T. Kennedy, K. Alkassab, T. Huynh, M. Elmi, J. Martinez, S. Sawan and G. Rijal, *AIMS Microbiol.*, 2022, **8**, 239–277.

13 S. Sharma, J. Mohler, S. D. Mahajan, S. A. Schwartz, L. Bruggemann and R. Aalinkeel, *Microorganisms*, 2023, **11**, 1614.

14 M. M. Zafer, G. A. Mohamed, S. R. M. Ibrahim, S. Ghosh, C. Bornman and M. A. Elfaky, *Arch. Microbiol.*, 2024, **206**, 101.

15 G. Ferreres, A. Bassegoda, J. Hoyo, J. Torrent-Burgués and T. Tzanov, *ACS Appl. Mater. Interfaces*, 2018, **10**, 40434–40442.

16 J. Park, A. Nabawy, J. Doungchawee, N. Mahida, K. Foster, T. Jantarat, M. Jiang, A. N. Chattopadhyay, M. A. Hassan, D. K. Agrohia, J. M. Makabenta, R. W. Vachet and V. M. Rotello, *ACS Appl. Mater. Interfaces*, 2023, **15**, 37205–37213.

17 R. Dey, S. Mukherjee, R. Mukherjee and J. Haldar, *Chem. Sci.*, 2024, **15**, 259–270.

18 K. R. Rouillard, O. P. Novak, A. M. Pistiolis, L. Yang, M. J. R. Ahonen, R. A. McDonald and M. H. Schoenfisch, *ACS Infect. Dis.*, 2021, **7**, 23–33.

19 T. Yang, A. N. Zelikin and R. Chandrawati, *Adv. Sci.*, 2018, **5**, 1701043.

20 S. K. Kutty, N. Barraud, A. Pham, G. Iskander, S. A. Rice, D. S. Black and N. Kumar, *J. Med. Chem.*, 2013, **56**, 9517–9529.

21 L. M. Estes Bright, M. K. Chug, S. Thompson, M. Brooks, E. J. Brisbois and H. Handa, *J. Biomed. Mater. Res.*, 2024, **112**, e35442.

22 L. Y. Hardefeldt and J. F. Prescott, in *Antimicrobial Therapy in Veterinary Medicine*, 2024, pp. 143–167, DOI: [10.1002/9781119654629.ch8](https://doi.org/10.1002/9781119654629.ch8).

23 S. B. Chaudhry, M. P. Veve and J. L. Wagner, *Pharmacy*, 2019, **7**, 103.

24 L. M. Estes Bright, M. R. S. Garren, M. Douglass and H. Handa, *ACS Appl. Mater. Interfaces*, 2023, **15**, 15185–15194.

25 J. Murugaiyan, P. A. Kumar, G. S. Rao, K. Iskandar, S. Hawser, J. P. Hays, Y. Mohsen, S. Adukkadukkam, W. A. Awuah, R. A. Jose, N. Sylvia, E. P. Nansubuga, B. Tilocca, P. Roncada, N. Roson-Calero, J. Moreno-Morales, R. Amin, B. K. Kumar, A. Kumar, A.-R. Toufik, T. N. Zaw, O. O. Akinwotu, M. P. Satyaseela and M. B. M. van Dongen, *Antibiotics*, 2022, **11**, 200.

26 E. J. Brisbois, H. Handa, T. C. Major, R. H. Bartlett and M. E. Meyerhoff, *Biomaterials*, 2013, **34**, 6957–6966.

27 Y. Wu, L.-C. Xu, E. Yeager, K. G. Beita, N. Crutchfield, S. N. Wilson, P. Maffe, C. Schmiedt, C. A. Siedlecki and H. Handa, *Acta Biomater.*, 2024, **180**, 372–382.

28 R. G. Maset, A. Hapeshi, J. Lapage, N. Harrington, J. Littler, S. Perrier and F. Harrison, *NPJ Biofilms Microbiomes*, 2023, **9**, 36.

29 J. Pant, M. J. Goudie, S. P. Hopkins, E. J. Brisbois and H. Handa, *ACS Appl. Mater. Interfaces*, 2017, **9**, 15254–15264.

30 Y. Zhou, J. Tan, Y. Dai, Y. Yu, Q. Zhang and M. E. Meyerhoff, *Chem. Commun.*, 2019, **55**, 401–404.

31 Y. Zhou, Q. Zhang, J. Wu, C. Xi and M. E. Meyerhoff, *J. Mater. Chem. B*, 2018, **6**, 6142–6152.

32 A. Brizzolari, M. Dei Cas, D. Cialoni, A. Marroni, C. Morano, M. Samaja, R. Paroni and F. M. Rubino, *Molecules*, 2021, **26**, 4569.

33 J. Sun, X. Zhang, M. Broderick and H. Fein, *Sensors*, 2003, **3**, 276–284.

34 C. W. McCarthy, J. Goldman and M. C. Frost, *ACS Appl. Mater. Interfaces*, 2016, **8**, 5898–5905.

35 J. Cheng, K. He, Z. Shen, G. Zhang, Y. Yu and J. Hu, *Front. Chem.*, 2019, **7**, 530.

36 A. R. Ketchum, A. K. Wolf and M. E. Meyerhoff, *J. Lab. Chem. Educ.*, 2017, **5**, 79–85.

37 N. J. Snyder, L. B. Tabas, D. M. Berry, D. C. Duckworth, D. O. Spry and A. H. Dantzig, *Antimicrob. Agents Chemother.*, 1997, **41**, 1649–1657.

38 B. J. Privett, S. M. Deupree, C. J. Backlund, K. S. Rao, C. B. Johnson, P. N. Coneski and M. H. Schoenfisch, *Mol. Pharmaceutics*, 2010, **7**, 2289–2296.

39 A. G. Abdelhamid and A. E. Yousef, *Antibiotics*, 2023, **12**, 1005.

40 A. Dey, M. Yadav, D. Kumar, A. K. Dey, S. Samal, S. Tanwar, D. Sarkar, S. K. Pramanik, S. Chaudhuri and A. Das, *Chem. Sci.*, 2022, **13**, 10103–10118.

41 A. Zhao, J. Sun and Y. Liu, *Front. Cell. Infect. Microbiol.*, 2023, **13**, 1137947.

42 B. L. Prosser, D. Taylor, B. A. Dix and R. Cleeland, *Antimicrob. Agents Chemother.*, 1987, **31**, 1502–1506.

43 M. I. El-Assal and N. G. El-Menofy, *Int. J. Pharm. Pharm. Sci.*, 2019, **11**, 14–27.

44 F. Bu, X. Kang, D. Tang, F. Liu, L. Chen, P. Zhang, W. Feng, Y. Yu, G. Li, H. Xiao and X. Wang, *Bioact. Mater.*, 2024, **33**, 341–354.

